HHS Public Access

Author manuscript

ACS Appl Mater Interfaces. Author manuscript; available in PMC 2016 December 30.

Published in final edited form as:

ACS Appl Mater Interfaces. 2015 December 30; 7(51): 28665–28672. doi:10.1021/acsami.5b10589.

Micro and Nano-patterned Topographical Cues for Regulating Macrophage Cell Shape and Phenotype

Thuy U. Luu[1,2], **Shannon C. Gott**[3], **Bryan W. K. Woo**[3], **Masaru P. Rao**[3,4,5], and **Wendy F. Liu**[2,6,7,*]

[1]Department of Pharmacological Sciences, University of California at Irvine

[2]The Edwards Lifesciences Center for Advanced Cardiovascular Technology, University of California at Irvine

[3]Department of Mechanical Engineering, University of California at Riverside

[4]Department of Bioengineering, University of California at Riverside

[5]Materials Science and Engineering Program, University of California at Riverside

[6]Department of Biomedical Engineering, University of California at Irvine

[7]Department of Chemical Engineering and Materials Science, University of California at Irvine

Abstract

Controlling the interactions between macrophages and biomaterials is critical for modulating the response to implants. While it has long been thought that biomaterial surface chemistry regulates the immune response, recent studies have suggested that material geometry may in fact dominate. Our previous work demonstrated that elongation of macrophages regulates their polarization towards a pro-healing phenotype. In this work, we elucidate how surface topology might be leveraged to alter macrophage cell morphology and polarization state. Using a deep etch technique, we fabricated titanium surfaces containing micro and nano-patterned grooves, which have been previously shown to promote cell elongation. Morphology, phenotypic markers, and cytokine secretion of murine bone marrow derived macrophages on different groove widths were analyzed. The results suggest that micro and nano-patterned grooves influenced macrophage elongation, which peaked on substrates with 400-500 nm wide grooves. Surface grooves did not affect inflammatory activation, but drove macrophages towards an anti-inflammatory, pro-healing phenotype. While secretion of TNF-alpha remained low in macrophages across all conditions, macrophages secreted significantly higher levels of anti-inflammatory cytokine, IL-10, on intermediate groove widths compared to cells on other Ti surfaces. Our findings highlight the potential of using surface topography to regulate macrophage function, and thus control the wound healing and tissue repair response to biomaterials.

Keywords

macrophage polarization; topography; groove; biocompatibility; titanium

[*]**Corresponding Author** Address: University of California Irvine, 2412 Engineering Hall, Irvine, CA 92697, Tel.: +1 949 824 1682; fax: +1 949 824 9968, wendy.liu@uci.edu.

1. Introduction

Implantation of a biomaterial-containing device is an essential component of many therapies used in modern medicine,[1] and although medical devices have significantly advanced in complexity and functionality, the host response to the biomaterial itself is still a major concern for the longevity of most devices. This foreign body response begins with injury to the tissue caused by surgical implantation, and is followed by inflammatory cell infiltration and activation, and finally the formation of a fibrous capsule to isolate the implant. It is thought that macrophages, immune cells that regulate inflammatory and wound healing processes, are a key determinant of the overall response to the foreign material.[2] Macrophages are highly plastic cells that are involved in host defense, wound healing, and immune regulation. To perform these diverse functions, they polarize towards different phenotypes in response to cues in their microenvironment. For example, in response to inflammatory or danger signals including lipopolysaccharide or interferon-γ (IFN-γ) macrophages secrete pro-inflammatory cytokines, such as tumor necrosis factor-α (TNF-α) and express inducible nitric oxide synthase (iNOS) to fight infection. In contrast, in a wound-healing environment, they produce anti-inflammatory mediators, such as interleukin 10 (IL-10) and arginase-1 (Arg1) to facilitate tissue repair.[3-4] Understanding how biomaterials regulate the phenotypic polarization of macrophages will likely aid the design of biomaterials for medical devices.

It has conventionally been thought that the chemistry of biomaterials dictates the behavior of infiltrating immune cells by altering cell adhesive interactions. However, recent evidence suggests that material geometry, or size and shape, may in fact dominate the overall response.[5-7] Biomaterial surface micro-topography has also been explored as physical cue to control the host response, and offers the advantage of long-term stability and cost-effective fabrication methods. Studies have generally suggested that surfaces that contain micro-scale features appeared to enhance the adhesion of macrophages and their secretion of inflammatory cytokines including IL-1β, IL-6, and nitric oxide when compared to macrophages on smooth surfaces.[8-11] More recently, it has been suggested that the degree of roughness is important, since TiO_2 surfaces that were moderately roughened induced polarization towards a pro-healing phenotype, whereas greater roughness led to inflammatory activation.[5] Precisely engineered microfabricated substrates have further helped to elucidate the effects of topography on macrophage behavior and the host response. Lithographically generated gratings as well as different post geometries have also been shown to modulate macrophage TNF-α and vascular endothelial growth factor (VEGF) secretion.[12,13] Finally, using electrospinning to create three-dimensional micro- or nano-scale fibers, it has been observed that nanofibers elicit significantly less macrophage adhesion and inflammatory activation, and minimize the host response, when compared to microfibers.[14-16] Taken together, these studies suggest that micro and nano-patterned topographies modulate macrophage behavior in vitro as well as the host response in vivo. However, the mechanism underlying topography-induced changes in macrophage function is still not well understood.

We recently demonstrated that cell shape is involved in regulating macrophage polarization state.[17] Specifically macrophages forced to elongate on fibronectin micropatterned lines exhibited an increase in expression of M2 polarization markers. Cell elongation influences the behavior of many cell types, particularly myocytes, which rely on their shape for directional force generation.[18-20] While the function of macrophages in the body is quite different, these cells have been shown to exhibit different shapes in vivo, where M2 polarized cells are more elongated and often found within fibrous tissue architectures.[21-23] Immune cells may in fact share similar mechanisms with other cell types for sensing their extracellular environment. Elongated cells generally exhibit focal adhesions that are aligned along the direction of elongation and a more organized cytoskeletal components.[24-27] While macrophages do not form extensive focal adhesions, phalloidin staining of the actin cytoskeleton of M2 polarized or micropatterned macrophages is indeed brighter.[17] Furthermore, a growing body of evidence in the stem cell field suggest that physical features on the culture substrate regulate differentiation through changes adhesion signaling and cytoskeletal organization.[28-31] As such, it is possible that changes in macrophage behavior from surface topographies may also depend on a mechanism involving changes in cell shape and adhesion.

In this study, we hypothesized that surface topography alters macrophage function through control of cell shape. To test this, we examined the effect of surface grooves on macrophage cell elongation and polarization. Using deep-etch techniques, we fabricated titanium surfaces containing micro and nano-patterned grooves, which have been previously shown to promote bone marrow stromal and endothelial cells to elongate and regulate cell function.[32-33] We characterized the degree of macrophage elongation resulting from adhesion to a range of groove widths and examined the expression of phenotypic markers, as well as secretion of cytokines. The results demonstrate that elongation and degree of M2 polarization are correlated, and suggest a promising approach for modulating macrophage function in response to biomaterial implants by using structured immunomodulatory surfaces.

2. Experimental Section

2.1 Patterned Ti substrate design and fabrication

Titanium substrates were fabricated as previously described.[33] Briefly, polished Grade 1 Ti substrates were cleaned thoroughly by sequential sonication in acetone and isopropanol, followed by rinsing in deionized water, and drying with N_2 gas. A SiO_2 etch mask was deposited using plasma-enhanced chemical vapor deposition (VLR, Unaxis), followed by thermoplastic resist spin-coating. Patterns were transferred from a silicon nanoimprint master to the resist using thermal nanoimprint lithography (NX2000, Nanonex). The patterns were transferred into the SiO_2 mask layer by plasma-etching, and then the underlying Ti substrate by titanium deep reactive ion etching (Ti DRIE) (E620 R&D, Panasonic Factory Solutions).[34-35] Subsequent removal of the remaining SiO_2 from the patterned surface by plasma etching revealed the bare patterned Ti. Each 22 mm × 22 mm substrate contained sixteen discrete 25 mm^2 patterned regions, including a unpatterned region (i.e., Blank) that served as a control. The pattern groove width (D) was varied from 0.15 μm to 50 μm and the

pitch (P) was twice the groove width (Figure 1A). The groove depth ranged between 0.8 μm to 1.3 μm. While multiplexed Ti substrates containing all groove dimensions were used for most in vitro experiments, a separate set of 22 mm × 22 mm substrates was fabricated with a single groove width patterned across the entirety of the surface (i.e., 200 nm, 450 nm, 5 μm, 50 μm, or unpatterned), for use in the BMDM cytokine secretion experiments. Prior to all in vitro experiments, Ti substrates were sterilized by incubating in 70% ethanol for 30 min, sonicating for 5 min, and then washing thoroughly with sterile PBS.

2.2 Cell isolation and culture

Bone marrow cells were isolated from femurs of C57BL/6 mice (Jackson Laboratories). Cells were treated with ACK lysis buffer (Invitrogen) to remove red blood cells, centrifuged, and then resuspended and cultured in D10 media consisting of high glucose DMEM supplemented with 10% heat-inactivated FBS, 2 mM L-glutamine, 100 units/mL, 100 μg/mL streptomycin (all from Invitrogen), and 10% conditioned media containing macrophage colony stimulating factor (M-CSF) produced by CMG 12-14 cells[36] to induce differentiation to bone marrow derived macrophages (BMDMs). BMDMs were maintained at 37°C in a humidified 5% CO_2 incubator. On day 7 of culture, BMDMs were dissociated using Cell Dissociation Buffer (Invitrogen) and on average, 20 million BMDMs were obtained per femur. Day 7 BMDMs were seeded on Ti substrates, which were not pre-treated before seeding. After 4 h of culture to allow adhesion of cells, the Ti substrates were transferred to a new culture well with fresh D10 media and then cultured for an additional 24 h or 36 h. Substrates were washed thoroughly with sterile PBS to remove non-adherent cells prior to all assays. All protocols involving animals were approved by the Institutional Animal Care and Use Committee at the University of California Irvine prior to initiation of the study.

2.3 Scanning electron microscopy

Dissociated day 7 BMDMs were seeded at a density of 70,000 cells/cm^2 on Ti substrates. After 36 h of culture, samples were fixed with 2.5% glutaraldehyde (Electron Microscopy Sciences) for 1 h and washed thoroughly with PBS, followed by a graded series of ethanol for dehydration. Samples were chemically dried by submerging in a bath of hexamethyldisilazane (Sigma-Aldrich) for 5 min. Dried samples were sputter-coated with iridium (South Bay Technology Ion Beam Sputtering System) prior to imaging by scanning electron microscopy (FEI Quanta 3D FEG Dual Beam). All images were taken at 15 kV accelerating voltage, high vacuum with 30 μm aperture.

2.4 Cell shape and morphological analysis

Dissociated day 7 BMDMs were seeded at a density of 100,000 cells/cm^2 on Ti substrates. To assess cell shape and morphology, cells were incubated with 10 μM CellTracker Green CMFDA (5-Chloromethylfluorescein Diacetate) (Invitrogen) in serum-free DMEM at 37 °C in a humidified 5% CO_2 incubator for 45 min, and then transferred to fresh D10 media. After 30 min, the samples were washed thoroughly with sterile PBS before imaging. For analysis of cell morphology, cells were visualized using an Olympus inverted microscope with a 20× objective. The long axis and short axis of each cell were manually traced and measured using ImageJ software (National Institutes of Health). The long axis was

determined as the longest length of the cells and the short axis was defined as the length across the nucleus, perpendicular to the long axis. Elongation factor was calculated as the ratio of the long axis to the short axis. A hundred cells per condition across three separate biological experiments were examined.

2.5 Fluorescence staining and imaging

Dissociated day 7 BMDMs were seeded on Ti substrates at a density of 100,000 cells/cm^2 for Arg1 and iNOS staining and 30,000 cells/cm^2 for vinculin staining. Samples were fixed with 4% paraformaldehyde (Electron Microscopy Sciences) for 5 min, and washed thoroughly with PBS containing 0.05% Tween-20 (Sigma-Aldrich). To permeabilize cells, the samples were treated with 0.1% Triton X-100 (Sigma-Aldrich) in PBS for 5 min, washed, and then blocked with 5% normal goat or donkey serum (Jackson ImmunoResearch) in PBS overnight at 4°C. Cells stained with arginase I (Arg1) were fixed with 100% cold methanol on ice for 15 min. Cells were then incubated with primary antibodies including goat anti-arginase-I (Santa Cruz Biotechnology Inc.), rabbit anti-NOS2 (Santa Cruz Biotechnology Inc.), or mouse monoclonal hVIN-1 anti-vinculin antibody (Sigma Aldrich) for 1 h, washed thoroughly with 1% BSA, and then incubated with Alexa Fluor-594 donkey anti-goat, Alexa Fluor-594 goat anti-mouse or Alexa Fluor-488 goat anti-rabbit fluorescent secondary antibodies (Jackson ImmunoResearch) for 1 h. For analysis of actin, samples were incubated with Alexa Fluor-488 conjugated phalloidin (Invitrogen). All cells were counterstained with Hoechst 33342 dye (Invitrogen), washed thoroughly, and then imaged using an Olympus inverted microscope (for Arg1 and iNOS) or a Zeiss LSM780 confocal microscope with 63× oil objective (for actin and vinculin). For fluorescence intensity analysis, sets of nuclear and Arg1 fluorescence images or nuclear and iNOS fluorescence images were taken of each sample and the integrated fluorescence intensity was quantified using CellProfiler software (MIT Broad Institute). Cells were determined to be positive for Arg1 or iNOS staining if integrated fluorescence for each cell exceeded a threshold value chosen such that more than 95% of non-stimulated cells on glass substrates were negative. At least three hundred cells per condition were examined across three separate biological experiments.

2.6 Cytokine secretion

BMDMs were cultured on Ti substrates as described above. In addition, cells were cultured on glass substrates and stimulated with a combination of *E.coli* LPS (Sigma-Aldrich), recombinant murine IFN-γ (R&D systems, Minneapolis, MN), IL-4 (Invitrogen) and IL13 (Invitrogen) with concentrations as described in the Figure legends. Dissociated day 7 BMDMs were seeded at a density of 100,000 cells/cm^2 on Ti and glass substrates. After an additional 36 h, supernatants were collected and analyzed for TNF-α and IL-10 by ELISA (enzyme-linked immunosorbent assay) following the manufacturer's instructions (BioLegend, San Diego, CA). Three separate biological experiments were performed.

2.7 Statistical analyses

Statistical analysis was performed using ordinary one-way ANOVA with Dunnett's post hoc test and uncorrected Fisher's LDS (multiple comparisons test). $p<0.05$ was considered statistically significant.

3. Results

3.1 Micro and nano-patterned grooves regulate macrophage elongation

Titanium (Ti) substrates were fabricated with highly defined and uniform patterned surface topographies, as demonstrated by scanning electron microscopy (SEM) (Figure 1B). Measurements of grooves using SEM micrographs confirmed that the groove width and pitch, or distance between grooves, were achieved as designed. Macrophages seeded on Ti materials adhered and spread to a flat, pancake shape on unpatterned surfaces after 36 h of culture (Figure 1B). Consistent with previous observations in other cell types as well as macrophage cell lines,[12, 26, 37] bone marrow derived macrophages aligned along the grooved surface topographies, generally in the direction parallel to the grooves (Figure 1B). We observed that compared to cells on the unpatterned surfaces, many cells on the patterned surfaces appeared to be less flattened, which was accentuated on surfaces with grooves smaller than 5 μm wide (Figure 1B). Cell elongation appeared to be most dramatic on substrates with 450 nm wide groves (Figure 1B).

In order to more quantitatively assess cell shape and allow better detection of the cell borders, we used Cell Tracker Green (CMFDA) to fluorescently label cells, and examined their shape by fluorescent light microscopy (Figure 2A). Macrophages were seeded on titanium surfaces with groove widths ranging from 150 nm to 50 μm. Similar to the images taken by SEM, fluorescent images of macrophages also showed alignment along the length of the grooves, with cells exhibiting the highest degree of elongation along the 400-500 nm grooves. The degree of elongation was determined by measuring the length of the longest axis and dividing by the width across the cell nucleus, and revealed a biphasic dependence of elongation on groove width. Compared to blank Ti substrate, widths, that were in a range between 200 nm and 10 μm, led to higher cell alignment and significant higher elongation factor (Figure 2B). The highest degree of elongation was observed on surfaces with grooves of approximately 450-500 nm wide (Figure 2B). The degree of cell spreading was similar and averaged approximately 550-750 μm^2 across all groove widths (Figure 2C). Together, these data suggested that surface grooves on titanium surfaces influence macrophage elongation without altering spread cell area.

3.2 Surface grooves alter adhesive and cytoskeletal structure

To more closely examine the interactions between macrophages and grooved Ti substrates, we evaluated adhesive structures and actin filaments using fluorescent microscopy. Macrophages were cultured on 200 nm, 450 nm, 5 μm, 50 μm patterned surfaces and non-patterned surfaces and analyzed for vinculin by immunostaining and actin by phalloidin binding (Figure 3). Consistent with what we and others have previously observed, macrophages do not exhibit organized stress fibers. Instead, the cells exhibited diffuse actin staining with some clustering particularly at the tips of elongated cells on 450 nm and 5 μm

grooves. Well spread cells also showed actin clusters within lamellepodia. Vinculin staining revealed similarly diffuse structures with few focal adhesions. Interestingly, cells cultured on 200 nm grooved surfaces exhibited few structures containing actin clusters and less overall vinculin staining, suggesting that 200 nm grooves may in fact depress adhesive interactions. Together, these data demonstrate that although adhesive and cytoskeletal structures in macrophages are relatively disorganized compared to other adhesive cell types including fibroblasts and endothelial cells, surface grooves do alter these structures.

3.2 Surface grooves modulate macrophage phenotype

We previously reported that BMDM cell shape influences their phenotype, and specifically that cells forced to elongate on micropatterned lines increased expression of phenotypic markers associated with the alternatively activated, M2 phenotype. We anticipated that since surface grooves alter macrophage cell shape, they might also be leveraged to modulate phenotype. To investigate this, we examined arginase-1 (Arg1, anti-inflammatory marker) and inducible nitric oxide synthase (iNOS, inflammatory marker) expression by immunofluorescence microscopy. Expression levels were compared against control cells polarized by cytokine treatment. We found that in comparison to IL-4/IL- 13 treatment, the expression of Arg1 on titanium surfaces was lower, but varied and dependent on groove dimensions (Figure 4B). At very small groove widths, expression of Arg1 was low, and increasing the groove width led to an increase in Arg1 expression peaking broadly on substrates containing 400 nm - 5 μm grooves (Figure 4B). Arg1 expression in cells on 300 nm, 500 nm, 1 μm, 2.5 μm, 5 μm, and 10 μm grooves was significantly different from expression in cells on 150 nm grooves. The expression of Arg1 was generally correlated with the degree of elongation, although at wider groove dimensions (25 – 50 μm) and flat titanium surfaces where elongation was generally lower, the Arg1 expression remained relatively high. The expression of iNOS remained similarly low across all groove widths (Figure 4D) and much less than macrophages stimulated towards an M1 phenotype by treatment with 10 ng/mL LPS and 10 ng/mL IFN-γ. Thus, these data suggested that surface grooves on Ti do not affect inflammatory activation, but drive macrophages to polarize towards an anti-inflammatory, pro-healing phenotype.

To further investigate whether grooves altered the secretion of cytokines associated with phenotypic polarization, we examined levels of IL-10 and TNF-α, representative anti- and pro- inflammatory cytokines respectively in the media after macrophages were cultured on Ti substrates containing single grooved patterns including 200 nm, 450 nm, 5 μm or 50 μm grooves, as well as an unpatterned control Ti surface. We found macrophages cultured on 5 μm surfaces exhibited significantly higher secretion of the anti-inflammatory cytokine, IL-10, when compared to cells on other Ti surfaces (Figure 5A). In comparison, secretion of TNF-α remained low in macrophages across all conditions (Figure 5B). Together, these data show that for Ti substrates, grooved surfaces can indeed modulate the function of macrophages, promoting an anti-inflammatory phenotype.

4. Discussion

We demonstrate the effect of grooved topographies on bone marrow derived macrophage shape, phenotypic markers, and cytokine secretion. Our results show that for Ti substrates, micro and nano-grooved topographies caused macrophages to elongate along the direction of the grooves, consistent with previous studies with other cell types on similar substrates.[32-33] Interestingly, the degree of cell elongation level was biphasic and decreased when cells were cultured on grooves less than 200 nm or greater than 10 μm. When the grooves were too narrow, cells did not elongate likely because adhesions could not form. When the grooves were too wide grooves, most cells also did not elongate as they tended to spread in the flat regions, but a few elongated cells were observed along the edge of the grooves. These data suggest that for Ti substrates, there is a minimum groove width that is necessary for cells to elongate, and that wider grooves lead cells to spread in all directions on the flat regions with minimal elongation. The total extent of cell spreading, as measured by the spread cell area, was consistent across substrates with different groove sizes, suggesting that changes in elongation were not caused by an inhibition or enhancement of overall cell spreading.

We found that Ti surface topography regulates polarization-associated macrophage markers, and moderately but significantly affect their release of cytokines. In our previous work, we demonstrated that geometry of cell adhesion influences macrophage phenotype.[17] The results from the current study corroborate with our previous work and show that macrophage Arg1 expression and IL-10 secretion was modulated by cell elongation, and depended on groove size. Our study did not distinguish between specific alternative activation phenotypes (M2a, M2b, and M2c), which is an important area of future investigation. Moreover, these results were obtained in calcium-containing DMEM media, and further studies using alternative media may help to elucidate a potential role for calcium, which has previously been shown to impact macrophage inflammatory activation. [38] Interestingly, the degree of Arg1 expression was somewhat elevated on substrates with wider groove sizes, even though the average cell elongation was not elevated relative to unpatterned blank surfaces. It is possible that cells that elongate along the 1 μm high edge of the grooves promote an overall alternatively-activated polarization response through paracrine effects. In particular, few elongated cells polarized towards an anti-inflammatory phenotype could in turn influence the behavior of neighboring non-elongated cells.[4] Moreover, surface topography did not affect on the expression of iNOS and TNF-α, markers of macrophage inflammatory M1 polarization. Together, these data demonstrated that for Ti substrates, surface grooves help polarize macrophages toward an anti-inflammatory, pro-healing phenotype independent of exogenous cytokine stimulation.

Grooved surfaces have been shown to modulate adhesion, adhesion signaling, and cytoskeletal organization of many cell types including fibroblasts, myocytes, epithelial cells, and mesenchymal stem cells. The size of focal adhesions in epithelial cells, as detected by immunostaining of vinculin, is often directly correlated with groove width, and increased from 400 nm to 1500 nm as grooves on Si substrates were increased from 330 nm to 2100 nm and were 600 nm deep.[25] Grooved substrates also lead to changes in integrin expression and focal adhesion kinase (FAK) phosphorylation.[29] While vinculin staining in

macrophages is not as intense, as shown by our own work and others,[39-41] our data show that on very narrow 200 nm wide grooves where macrophages were not elongated, adhesion size appeared to be diminished relative to cells on other groove sizes and flat substrates. In addition, our results show that macrophage elongation influences the organization of actin cytoskeletal components, since the intensity of phalloidin staining was higher in elongated cells. These data show that while macrophages do not appear to exhibit highly organized cytoskeletal and adhesive structures when compared to other groove-sensitive cell types, topographical substrates are capable of modulating these cellular components, and may indeed play an important role in regulating macrophage polarization.

Understanding how physical cues presented by biomaterial surfaces regulates macrophage adhesion and polarization will have important implications for medical device design. While biomaterial chemistry has long been thought to regulate macrophage response, to date less is known about how physical cues might regulate macrophage function. Our data suggest that surface topographies that modulate macrophage cell shape, for example microscale grooves, may be used to regulate macrophage behavior and specifically their activation towards a pro-healing alternatively activated M2 phenotype. Given the important role of macrophages in wound healing and tissue repair, this may provide a simple method for regulating the host response to biomaterial implants. While the current work has been focused on two-dimensional biomaterial surfaces, it is likely that three-dimensional scaffolds that present topographical cues including fibrous tissue architectures may similarly alter macrophage function and the wound healing response. Moreover, further studies using human cells will be necessary to unveil the true translational potential of topography-mediated macrophage polarization and wound healing. Ultimately, controlling the immune response to 3D biomaterial architecture may be useful for leveraging immune-mediated healing in tissue engineering and regenerative medicine.[42]

5. Conclusions

We demonstrate that micro and nano-patterned surface groove cues regulate macrophage elongation and phenotype polarization. Using deep-etched titanium surfaces with a wide range of groove sizes (150 nm to 50 μm), we found that BMDM elongation and expression of phenotypic markers associated with a pro-healing M2 phenotype was highest on intermediate groove sizes ranging from 400 nm to 5 μm in width. Collectively, these results highlight the potential utility of groove patterned materials to promote wound healing in response to biomaterial implants.

ACKNOWLEDGEMENTS

We thank L. McCarthy for technical assistance in the laboratory, Adeela Syed for technical assistance in the Optical Biology Center, and the Lodoen laboratory for guidance with cell isolation and culture. This work was made possible, in part, through access to the confocal facility of the Optical Biology Shared Resource of the Cancer Center Support Grant (CA-62203) at the University of California, Irvine.

Funding Sources

This work was supported by National Institutes of Health (NIH) National Institute of Dental and Craniofacial Research (NIDCR) Grant DP2DE023319 and the Edwards Lifesciences Fund. T. U. L. was supported by a California Institute of Regenerative Medicine (CIRM) Training Fellowship (TG2-01152). Patterned titanium

substrate fabrication was partially supported by National Science Foundation CAREER Grant CMMI-1254999, and a University of California, Riverside Collaborative Seed Grant. S.C.G. was supported by a National Science Foundation Graduate Research Fellowship.

REFERENCES

1. Hubbell JA, Langer R. Translating Materials Design to the Clinic. Nat. Mater. 2013; 12:963–966. [PubMed: 24150414]
2. Anderson JM, Rodriguez A, Chang DT. Foreign Body Reaction to Biomaterials Semin. Immunol. 2008; 20:86–100.
3. Wynn TA, Chawla A, Pollard JW. Macrophage Biology in Development. Homeostasis and Disease Nature. 2013; 496:445–455.
4. Martinez FO, Gordon S. The M1 and M2 Paradigm of Macrophage Activation: Time For Reassessment F1000Prime Rep. 2014; 6:13. [PubMed: 24669294]
5. Ma QL, Zhao LZ, Liu RR, Jin BQ, Song W, Wang Y, Zhang YS, Chen LH, Zhang YM. Improved Implant Osseointegration of a Nanostructured Titanium Surface via Mediation of Macrophage Polarization Biomaterials. 2014; 35:9853–9867. [PubMed: 25201737]
6. Veiseh O, Doloff JC, Ma M, Vegas AJ, Tam HH, Bader AR, Li J, Langan E, Wyckoff J, Loo WS, Jhunjhunwala S, Chiu A, Siebert S, Tang K, Hollister-Lock J, Aresta-Dasilva S, Bochenek M, Mendoza-Elias J, Wang Y, Qi M, Lavin DM, Chen M, Dholakia N, Thakrar R, Lacik I, Weir GC, Oberholzer J, Greiner DL, Langer R, Anderson DG. Size- and Shape-Dependent Foreign Body Immune Response to Materials Implanted in Rodents and Non-Human Primates. Nat. Mater. 2015; 14:643–651. [PubMed: 25985456]
7. Sridharan R, Cameron AR, Kelly DJ, Kearney CJ, O'Brien FJ. Biomaterial Based Modulation of Macrophage Polarization: A Review and Suggested Design Principles. Materials Today. 2015; 18:313–325.
8. Tan KS, Qian L, Rosado R, Flood PM, Cooper LF. The Role of Titanium Surface Topography on J774A.1 Macrophage Inflammatory Cytokines and Nitric Oxide Production. Biomaterials. 2006; 27:5170–5177. [PubMed: 16808973]
9. Refai AK, Textor M, Brunette DM, Waterfield JD. Effect of Titanium Surface Topography on Macrophage Activation and Secretion of Proinflammatory Cytokines and Chemokines. J. Biomed. Mater. Res. A. 2004; 70:194–205. [PubMed: 15227664]
10. Moura CCG, Zanetta-Barbosa D, Dechichi P, Carvalho VF, Soares PB. F. Effects of Titanium Surfaces on the Developmental Profile of Monocytes/Macrophages. Brazilian Dental Journal. 2014; 25:96–103. [PubMed: 25140712]
11. Bota PC, Collie AM, Puolakkainen P, Vernon RB, Sage EH, Ratner BD, Stayton PS. Biomaterial Topography Alters Healing In Vivo and Monocyte/Macrophage Activation In Vitro. J. Biomed. Mater. Res. A. 2010; 95:649–957. [PubMed: 20725970]
12. Chen S, Jones JA, Xu Y, Low HY, Anderson JM, Leong KW. Characterization of Topographical Effects on Macrophage Behavior in a Foreign Body Response. Model Biomaterials. 2010; 31:3479–3491.
13. Bartneck M, Schulte VA, Paul NE, Diez M, Lensen MC, Zwadlo-Klarwasser G. Induction of Specific Macrophage Subtypes by Defined Micro-Patterned Structures. Acta. Biomater. 2010; 6:3864–3872.
14. Cao H, McHugh K, Chew SY, Anderson JM. The Topographical Effect of Electrospun Nanofibrous Scaffolds on the In Vivo and In Vitro Foreign Body Reaction. J. Biomed. Mater. Res. A. 2010; 93:1151–1159. [PubMed: 19768795]
15. Saino E, Focarete ML, Gualandi C, Emanuele E, Cornaglia AI, Imbriani M, Visai L. Effect of Electrospun Fiber Diameter and Alignment on Macrophage Activation and Secretion of Proinflammatory Cytokines and Chemokines. Biomacromolecules. 2011; 12:1900–1911. [PubMed: 21417396]
16. Garg K, Pullen NA, Oskeritzian CA, Ryan JJ, Bowlin GL. Macrophage Functional Polarization (M1/M2) in Response to Varying Fiber and Pore Dimensions of Electrospun Scaffolds. Biomaterials. 2013; 34:4439–4451. [PubMed: 23515178]

17. McWhorter FY, Wang T, Nguyen P, Chung T, Liu WF. Modulation of Macrophage Phenotype by Cell Shape. Proc. Natl. Acad. Sci. 2013; 110:17253–17258. [PubMed: 24101477]
18. Alford PW, Nesmith AP, Seywerd JN, Grosberg A, Parker KK. Vascular Smooth Muscle Contractility Depends on Cell Shape. Integr. Biol. 2011; 3:1063–1070.
19. Ryall KA, Bezzerides VJ, Rosenzweig A, Saucerman JJ. Phenotypic Screen Quantifying Differential Regulation of Cardiac Myocyte Hypertrophy Identifies CITED4 Regulation of Myocyte Elongation. J. Mol. Cell. Cardiol. 2014; 72:74–84. [PubMed: 24613264]
20. Ye GJ, Aratyn-Schaus Y, Nesmith AP, Pasqualini FS, Alford PW, Parker KK. The Contractile Strength Of Vascular Smooth Muscle Myocytes is Shape Dependent. Integr. Biol. 2014; 6:152–163.
21. Waldo SW, Li Y, Buono C, Zhao B, Billings EM, Chang J, Kruth HS. Heterogeneity of Human Macrophages in Culture and in Atherosclerotic Plaques. Am. J. Pathol. 2008; 172:1112–1126. [PubMed: 18321997]
22. Chinetti-Gbaguidi G, Baron M, Bouhlel MA, Vanhoutte J, Copin C, Sebti Y, Derudas B, Mayi T, Bories G, Tailleux A, Haulon S, Zawadzki C, Jude B, Staels B. Human Atherosclerotic Plaque Alternative Macrophages Display Low Cholesterol Handling but High Phagocytosis because of Distinct Activities of The Ppargamma and Lxralpha Pathways. Circ. Res. 2011; 108:985–995. [PubMed: 21350215]
23. Sharma VP, Beaty BT, Patsialou A, Liu H, Clarke M, Cox D, Condeelis JS, Eddy RJ. Reconstitution Of In Vivo Macrophage-Tumor Cell Pairing and Streaming Motility on One-Dimensional Micro-Patterned. Substrates Intravital. 2012; 1:77–85. [PubMed: 24634804]
24. Dalby MJ, Riehle MO, Yarwood SJ, Wilkinson CDW, Curtis ASG. Nucleus Alignment and Cell Signaling in Fibroblasts: Response to a Micro-Grooved Topography Exp. Cell Res. 2003; 284:272–280.
25. Teixeira AI, Abrams GA, Bertics PJ, Murphy CJ, Nealey PF. Epithelial Contact Guidance on Well-Defined Micro- and Nanostructured Substrates. J. Cell. Sci. 2003; 116:1881–1892. [PubMed: 12692189]
26. Yim EK, Pang SW, Leong KW. Synthetic Nanostructures Inducing Differentiation of Human Mesenchymal Stem Cells Into Neuronal Lineage Exp. Cell. Res. 2007; 313:1820–1829.
27. Kirmizidis G, Birch MA. Microfabricated Grooved Substrates Influence Cell-Cell Communication and Osteoblast Differentiation In Vitro Tissue. Eng. Part A. 2009; 15:1427–1436.
28. Engler AJ, Sen S, Sweeney HL, Discher DE. Matrix Elasticity Directs Stem Cell Lineage Specification. Cell. 2006; 126:677–689. [PubMed: 16923388]
29. Yim EK, Darling EM, Kulangara K, Guilak F, Leong KW. Nanotopography-Induced Changes in Focal Adhesions, Cytoskeletal Organization, and Mechanical Properties of Human Mesenchymal Stem Cells. Biomaterials. 2010; 31:1299–1306. [PubMed: 19879643]
30. Lee J, Abdeen AA, Zhang D, Kilian KA. Directing Stem Cell Fate on Hydrogel Substrates by Controlling Cell Geometry, Matrix Mechanics and Adhesion Ligand Composition. Biomaterials. 2013; 34:8140–8148. [PubMed: 23932245]
31. Kilian KA, Bugarija B, Lahn BT, Mrksich M. Geometric Cues for Directing the Differentiation of Mesenchymal Stem Cells. Proc. Natl. Acad. Sci. 2010; 107:4872–4877. [PubMed: 20194780]
32. Cipriano AF, Howitt ND, Gott SC, Miller C, Rao MR, Liu H. Bone Marrow Stromal Cell Adhesion and Morphology on Micro- and Sub-Micropatterned Titanium. J. Biomed. Nanotechnol. 2014; 10:660–668. [PubMed: 24734518]
33. Vandrangi P, Gott SC, Kozaka R, Rodgers VG, Rao MP. Comparative Endothelial Cell Response on Topographically Patterned Titanium and Silicon Substrates with Micrometer to Sub-Micrometer Feature Sizes. PLoS One. 2014; 9:e111465. [PubMed: 25357245]
34. Aimi MF, Rao MP, MacDonald NC, Zuruzi AS, Bothman DP. High-Aspect-Ratio Bulk Micromachining of Titanium. Nat. Mater. 2004; 3:103–105. [PubMed: 14743212]
35. Parker ER, Thibeault BJ, Aimi MF, Rao MP, MacDonald NC. Inductively Coupled Plasma Etching of Bulk Titanium for MEMS Applications. J. Electrochem. Soc. 2005; 152:C675–C683.
36. Morgado P, Ong YC, Boothroyd JC, Lodoen MB. Toxoplasma Gondii Induces B7-2 Expression Through Activation of JNK Signal Transduction. Infect. Immun. 2011; 79:4401–4412. [PubMed: 21911468]

37. Kulangara K, Adler AF, Wang H, Chellappan M, Hammett E, Yasuda R, Leong KW. The Effect of Substrate Topography on Direct Reprogramming of Fibroblasts to Induced Neurons. Biomaterials. 2014; 35:5327–5336. [PubMed: 24709523]

38. Pelegrin P, Surprenant A. Dynamics of Macrophage Polarization Reveal New Mechanism to Inhibit IL-1beta Release through Pyrophosphates. EMBO J. 2009; 28:2114–2127. [PubMed: 19536133]

39. Calle Y, Burns S, Thrasher AJ, Jones GE. The Leukocyte Podosome. Eur. J. Cell Biol. 2006; 85:151–157. [PubMed: 16546557]

40. Linder S. Invadosomes at a Glance. J. Cell Sci. 2009; 122:3009–3013.

41. Van Goethem E, Guiet R, Balor S, Charriere GM, Poincloux R, Labrousse A, Maridonneau-Parini I, Le Cabec V. Macrophage Podosomes Go 3D. Eur. J. Cell Biol. 2011; 90:224–236. [PubMed: 20801545]

42. Gott SC, Jabola BA, Rao MP. Vascular Stents with Submicrometer-Scale Surface Patterning Realized via Titanium Deep Reactive Ion Etching. J. Micromech. Microeng. 2015; 25:085016.

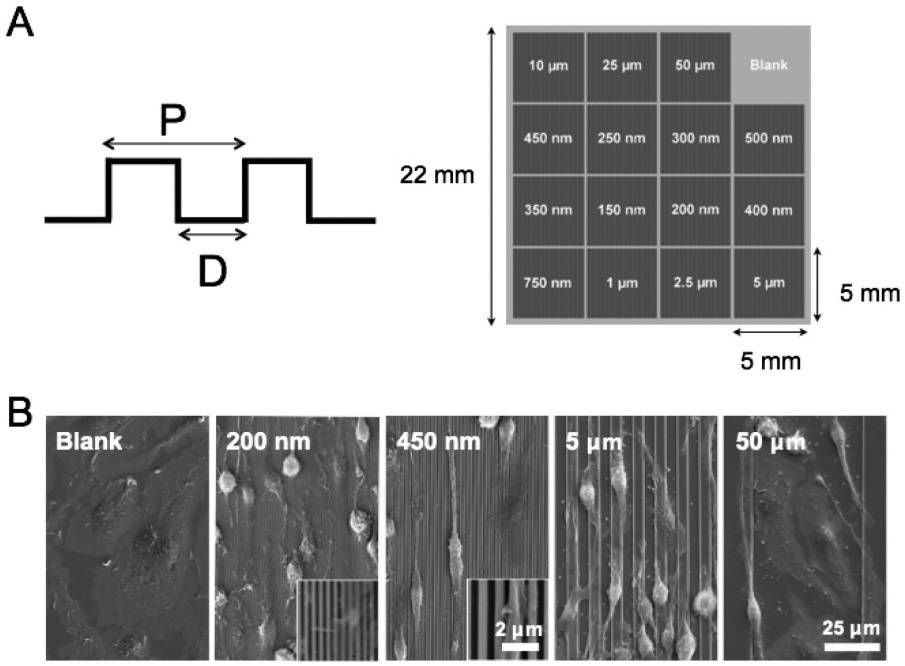

Figure 1. Deep-etched titanium surfaces with varied groove dimensions

(A) Schematic of the Ti substrate with micro- and nano-patterned surface topographies used in this study. D denotes groove width; P denotes pitch, which is twice the groove width. Groove depth is approximately 0.8 µm to 1.3 µm for all widths. **(B)** Scanning electron microscopy micrographs of BMDM after 36 h culture on Ti substrate with 200 nm, 450 nm, 5 µm, and 50 µm grating patterns and non-patterned control.

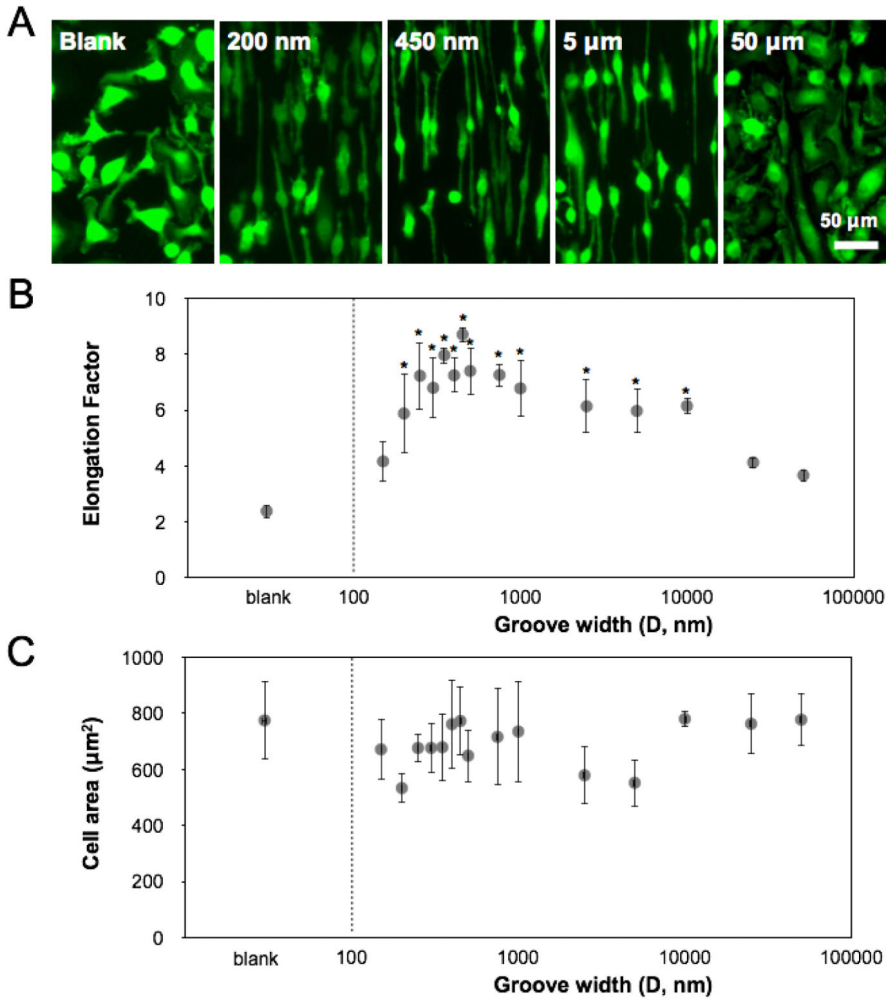

Figure 2. Grooved surfaces regulate macrophage elongation

(A) Fluorescence micrographs of BMDM after 24 h culture on bulk Ti substrate with 200 nm, 450 nm, 5 µm, and 50 µm grating patterns and non-patterned control. Cells were stained using CellTracker Green CMFDA dye for monitoring cell shape. Scale bar = 50 µm. **(B)** Quantification of BMDM elongation factor on Ti surfaces of varied groove widths. Mean ± SEM (*$p < 0.05$; ordinary one-way ANOVA with Dunnett's post test, in comparison to blank Ti substrate, $n = 3$). (**C**) Quantification of BMDM cell area on Ti surfaces of varied groove widths. Mean ± SEM, $n = 3$.

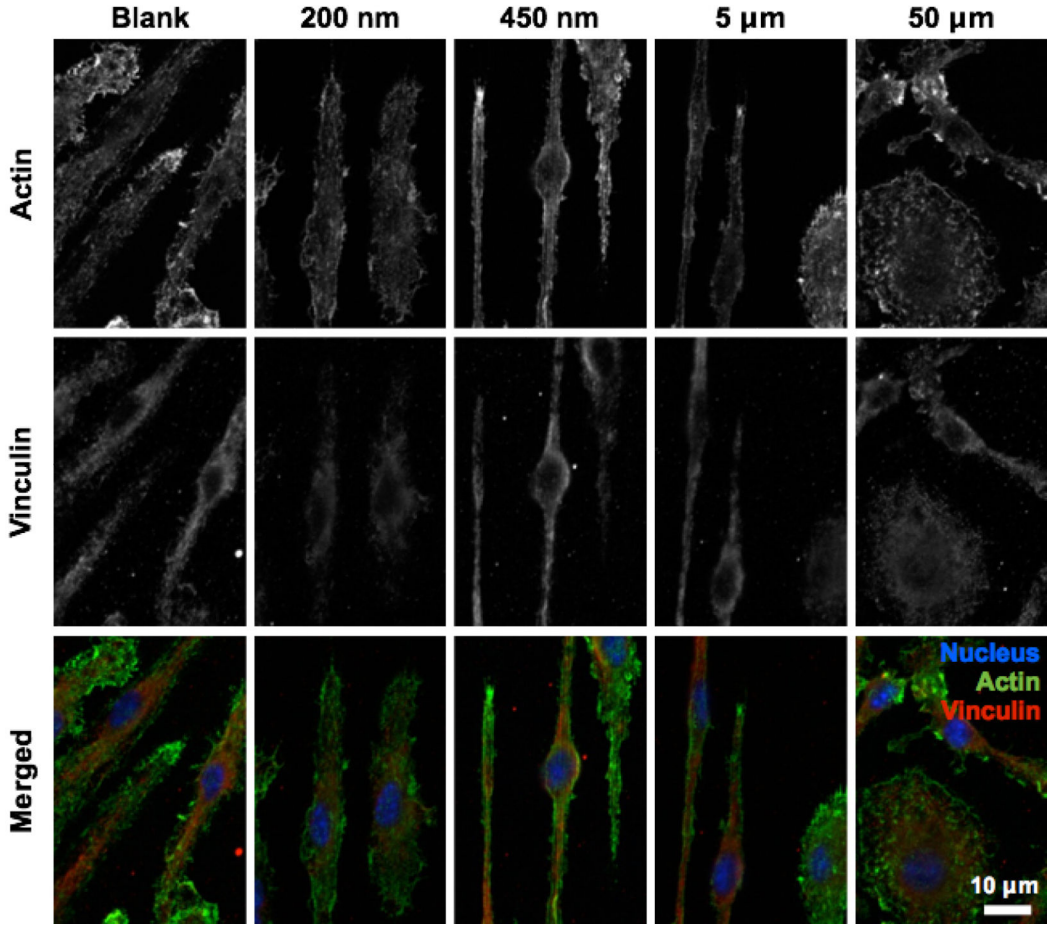

Figure 3. Adhesive and cytoskeletal structures of macrophages on grooved surfaces

Fluorescent images of vinculin (red; immunostaining) and actin filaments (green; phalloidin staining) in BMDMs cultured on various groove sizes.

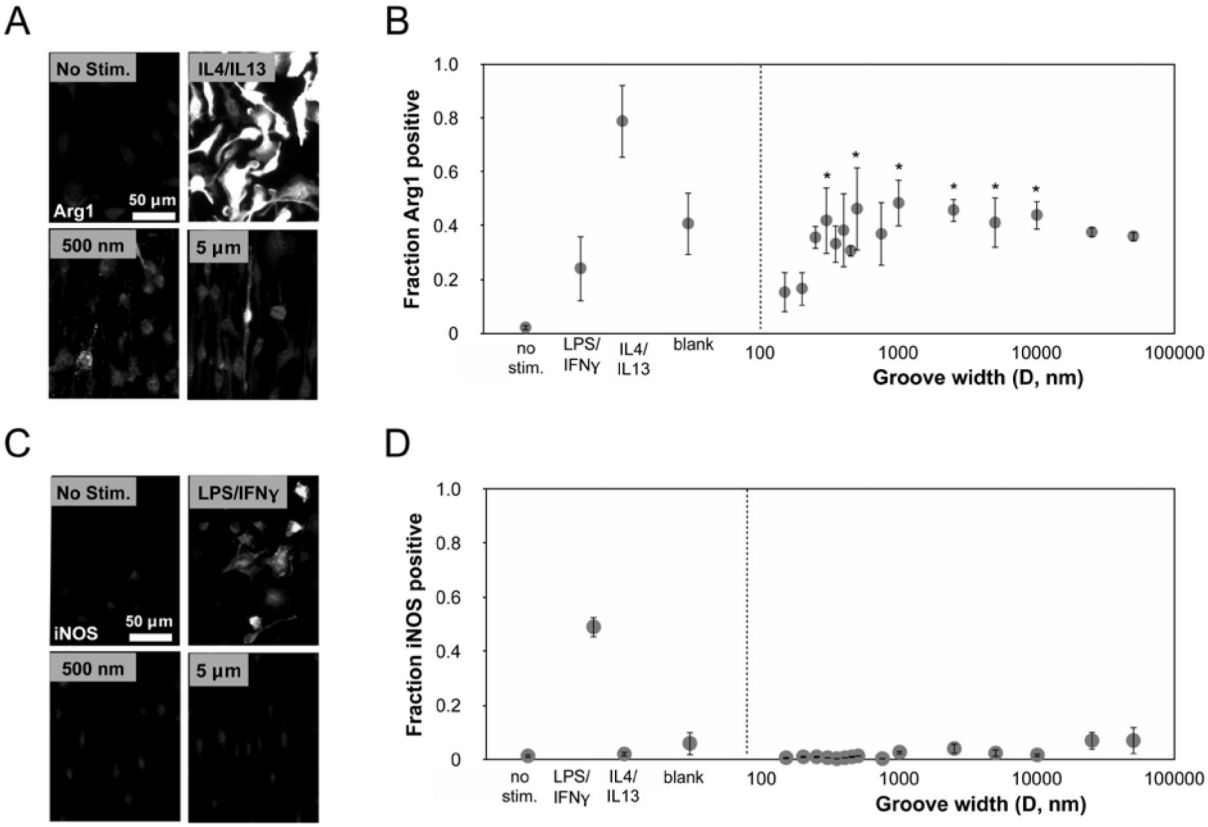

Figure 4. Expression of macrophage polarization markers on grooved surfaces

(**A**) Representative Arg1 immunofluorescent images of BMDMs on control and grooved substrates. Scale bar = 50 µm **(B)** Quantification of Arg1 expression corresponding to the groove width. Mean ± SEM (*p < 0.05; ordinary one-way ANOVA with uncorrected Fisher's LDS, blank and grooved surface topography substrates compared to 150 nm grooved substrate, *n* = 3). (**C**) Representative iNOS immunofluorescent images of BMDMs on control and grooved substrates. Scale bar = 50 µm. **(D)** Quantification of iNOS expression corresponding to the groove width. Mean ± SEM, *n* = 3. No stim. denotes unstimulated, LPS/IFN-γ was stimulated with 10 ng/mL LPS and 10 ng/mL IFN-γ, LPS/IL4/IL13 was stimulated with 20 ng/mL IL4 and 20 ng/mL IL13, Blank denotes unstimulated cells on a flat Ti substrate.

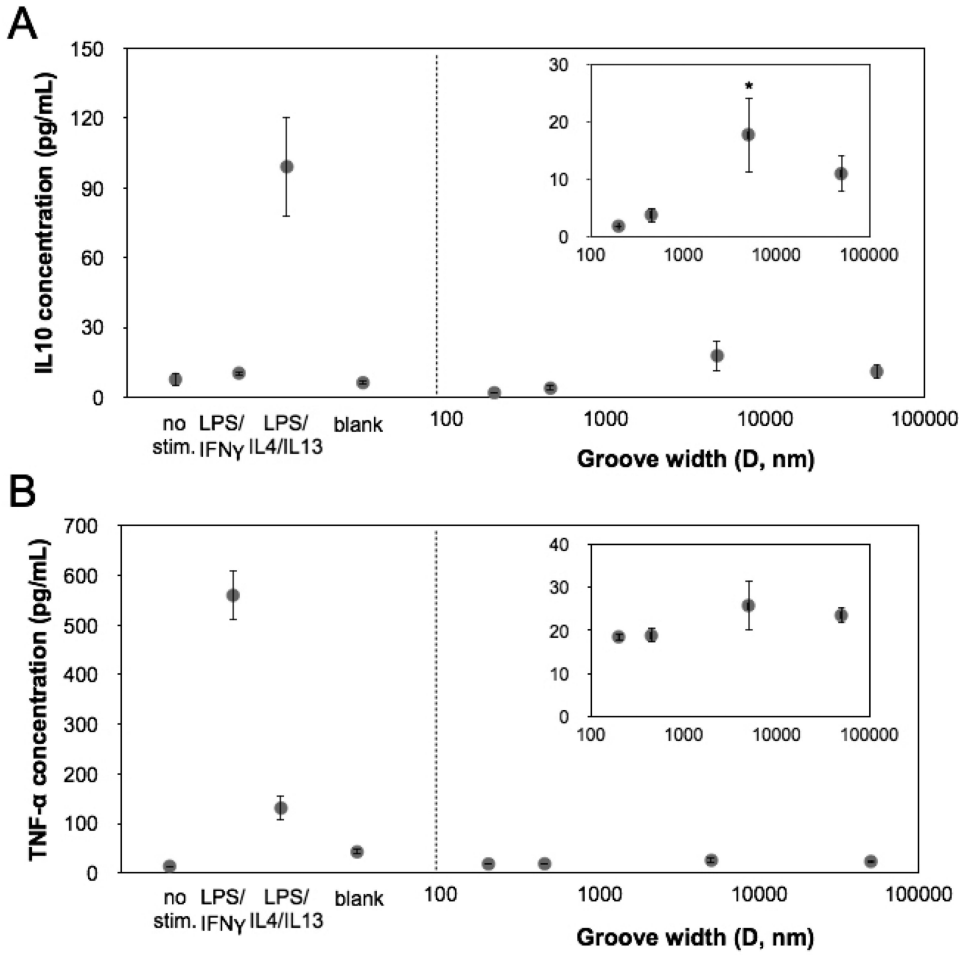

Figure 5. Cytokine secretion from macrophages on grooved surfaces

(A) Quantified IL10 secretion from macrophages cultured on different groove widths. Mean ± SEM (*$p < 0.05$; ordinary one-way ANOVA with Dunnett's post test, in comparison to 200 nm grooved substrate, $n = 3$). **(B)** Quantified TNF-α secretion from macrophages cultured on different groove widths. Mean ± SEM, $n = 3$. No stim. denotes unstimulated, LPS/IFN-γ was stimulated with 0.5 ng/mL LPS and 10 ng/mL IFN-γ, LPS/IL4/IL13 was stimulated with 0.5 ng/mL LPS, 20 ng/mL IL4 and 20 ng/mL IL13, Blank denotes unstimulated cells on a flat Ti substrate.